Photonic approach to the selective inactivation of viruses with a near-infrared subpicosecond fiber laser

Kong-Thon Tsen
Arizona State University
Department of Physics
P.O. Box 871504
Tempe, Arizona 85287

Shaw-Wei D. Tsen
Washington University School of Medicine
660 South Euclid Avenue
St. Louis, Missouri 63110

Q. Fu
Stuart M. Lindsay
Karen Kibler
Bert Jacobs
Arizona State University
Biodesign Institute
P.O. Box 871504
Tempe, Arizona 85287

T-C. Wu
B. Karanam
S. Jagu
Richard B. S. Roden
Chien-Fu Hung
The Johns Hopkins Medical Institutions
Department of Pathology
3400 North Charles Street
Baltimore, Maryland 21231

Otto F. Sankey
Arizona State University
Department of Physics
P.O. Box 871504
Tempe, Arizona 85287

B. Ramakrishna
Arizona State University
School of Material Sciences
P.O. Box 9309
Tempe, Arizona 85287

Juliann G. Kiang
Armed Forces Radiobiology Research Institute
Scientific Research Department
8901 Wisconsin Avenue
Bethesda, Maryland 20889-5603
    and
Uniformed Services University of the Health Sciences
Department of Medicine
    and
Department of Radiation Biology
4301 Jones Bridge Road
Bethesda, Maryland 20889-5603

Address all correspondence to: Kong-Thon Tsen, Department of Physics and Center for Biophysics, Arizona State University, Tempe, AZ 85287-1504. Tel: (480) 965-5206; E-mail: tsen@asu.edu

Abstract. We report a photonic approach for selective inactivation of viruses with a near-infrared subpicosecond laser. We demonstrate that this method can selectively inactivate viral particles ranging from nonpathogenic viruses such as the M13 bacteriophage and the tobacco mosaic virus to pathogenic viruses such as the human papillomavirus and the human immunodeficiency virus (HIV). At the same time, sensitive materials such as human Jurkat T cells, human red blood cells, and mouse dendritic cells remain unharmed. The laser technology targets the global mechanical properties of the viral protein shell, making it relatively insensitive to the local genetic mutation in the target viruses. As a result, the approach can inactivate both the wild and mutated strains of viruses. This intriguing advantage is particularly important in the treatment of diseases involving rapidly mutating viral species such as HIV. Our photonic approach could be used for the disinfection of viral pathogens in blood products and for the treatment of blood-borne viral diseases in the clinic. © 2009 Society of Photo-Optical Instrumentation Engineers. [DOI: 10.1117/1.3275477]

1 Introduction

Biochemical and pharmaceutical methods currently used for the inactivation of viral particles, although quite successful, encounter problems of drug resistance in the target virus. In addition, they also have clinical side effects. The ultraviolet (UV) disinfection method[1,2] is effective, however, UV lamps target both the nuclei acids and proteins, as a result they damage not only the viral particles but also the mammalian cells; in other words, it has no selectivity. In addition, UV irradiation raises concerns of mutation and has shadowing effects due to its relatively small penetration depth. The microwave absorption technique is not effective because most of the energy is transferred to the water and not to the target viral particle. Recently, a photochemical technique[3] was developed to disinfect blood supplies. However, potential risks and side effects have hindered its applications. A new method that circumvents these problems is therefore desirable.

In this paper, we report a photonic approach for selective inactivation of viruses with a near-IR subpicosecond laser. Our method with a near-IR ultrafast laser system, in contrast to the UV lamp technology, targets only the weak links on the protein shells of viral particles. By tuning to the appropriate laser power density, we demonstrate that it is feasible to damage the protein shells of viral particles leading to the inactivation of viral particles without harming the mammalian cells. Specifically, we demonstrate that this method can selectively
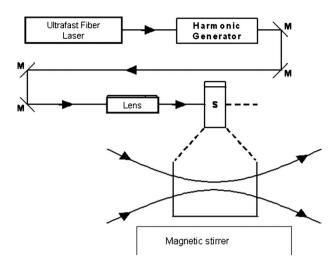
Fig. 1 Experimental setup for the inactivation of viral particles with a near-IR subpicosecond fiber laser:M, mirror; S, vial containing viruses in buffer solutions.

inactivate viral particles ranging from nonpathogenic viruses such as the M13 bacteriophage and the tobacco mosaic virus (TMV) to pathogenic viruses such as the human papillomavirus (HPV) and the human immunodeficiency virus (HIV), while sensitive materials such as human Jurkat T cells, human red blood cells, and mouse dendritic cells remain unharmed. In contrast to the UV lamp irradiation method, our photonic approach with a near-IR subpicosecond laser system not only provides selectivity but also minimizes shadowing effects (because penetration depth is much larger for the IR wavelength than for the UV wavelength).

2 Experimental Method, Samples, and Assays

2.1 Laser and Experimental Setup

The excitation source used in the inactivation of viruses was a compact, ultrashort pulsed fiber laser (with seed and amplifier, from Raydiance Inc.). As shown in Fig. 1, the ultrashort pulsed fiber laser, which has a wavelength of 1.55 μm, was operated at a repetition rate of 500 kHz and 5 μJ per laser pulse. The output of the second-harmonic generation (SHG) system of the fiber laser was used in the laser-irradiation experiments. It has a wavelength of 776 nm, about 1.4 μJ per laser pulse, a pulse width of full width at half maximum of about 600 fs, and a spectral width of about 70 cm^{-1}. Water, which usually coexists with biological microorganisms, absorbs radiation at 1.55 μm very severely, but is rather transparent in the near-IR and visible ranges. This is why the SHG beam was used. In all of our experiments, a single laser beam was used for the inactivation of viruses. A different laser power density was achieved by varying the average laser power and the size of the laser beam with an achromatic lens of long focal length. A magnetic stirrer (Corning Model: PC-420) was used to stir the viral sample in its buffer solution so as to facilitate the interaction of the laser with the viral particles. The duration of the laser irradiation was 2 h in all of our experiments. All the laser-irradiation experiments were carried out at $T=25$ °C. All the data are expressed in the form of (mean ± standard deviation).

2.2 Samples and Assays

2.2.1 For M13 bacteriophage

The VCSM13 Interference-Resistant Helper phage was purchased from Stratagene. To determine the infectivity of the helper phages from different batches, we diluted the phage to 10^3 plaque forming unit (pfu) in 50 μl of phosphate-buffered saline (PBS) and added the diluted phage to 1 ml of TG-1 *E. coli* growing at an OD 600 (optical density at 600 nm) of 0.4. The *E. coli* solution was then added into 3 ml of agarose top (10 g Bacto-Tryptone, 5 g yeast extract, 5 g NaCl, 1 g $MgCl_2 \cdot 6H_2O$, 7 g agarose in 1 l of water). After brief vortex, the mixture was poured evenly onto TYE plates (15 g Bacto-Agar, 8 g NaCl, 10 g Tryptone, 5 g yeast extract in 1 l of water) and cooled at room temperature until solidification. The plates were incubated at 37 °C overnight and plaques were counted on the next day. Plaque formation assay was performed in triplicate for each batch of phage. On another assay, we diluted the phage in serial amount from 10 to 10^3 pfu in 50 μl of PBS and added into 1 ml of TG-1 culture followed by plating as already described.

After overnight culture of TG-1 *E. coli* with helper phage on the agars plate, the discrete plaques was labeled and counted.

2.2.2 For HPV

HPV16 SEAP (secreated alkaline phosphatase) assay was performed as described earlier.[4]

Neutralization buffer was prepared by mixing DMEM (Dulbecco modified Eagle medium) without phenol red, 10% heat-inactivated FBS (fetal bovine serum), 1% nonessential amino acids, and 1% penicillin-streptomycin. The 293TT cells were plated 3 to 4 h before treatment in 96-well tissue-culture-treated flat-bottom plates at 30,000 cells/well in 100 μl neutralization buffer. Optiprep-purified HPV16 PV having SEAP as a reporter was diluted 1000-fold. At these dilutions, target cells typically generated enough SEAP for an output reading. The 100-μl pseudovirus treated with the laser was transferred onto the preplated cells and incubated for 68 to 72 h. At the end of the incubation, 40 μl of supernatant was harvested and clarified at $1500 \times g$ for 5 min. The SEAP content in the clarified supernatant was determined using p-nitrophenyl phosphate tablets (Sigma, St. Louis, Missouri) dissolved in diethanolamine, and absorbance was measured at 405 nm.

2.2.3 For HIV

HIV stocks [NL4-3, provided by the National Institutes of Health (NIH)] were diluted to 1×10^5 cpm/ml in DMEM (with no phenol red) for the laser-irradiation experiments.

U373-MAGI-CXCR4$_{CEM}$ cells (NIH AIDS Research & Reference Reagent Program) were seeded at 6×10^4 cells/ well in 24-well plates. To assay the infectivity of HIV, these cells were infected with samples, either laser-irradiated or not irradiated (control), at the indicated viral concentrations. Following a 48-h incubation, cells were fixed with a 1% paraformaldeyhde, 0.2% gluteraldehyde solution prepared in PBS. Fixed cells were washed twice with PBS and stained with a solution containing 0.4 mM potassium ferrocyanide,
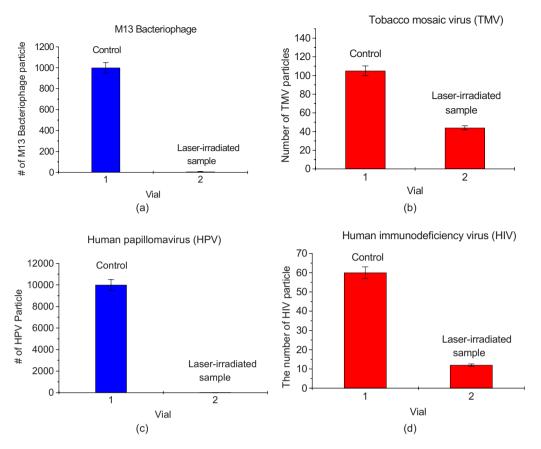
Fig. 2 Inactivation of viruses with a near-IR subpicosecond fiber laser for (a) M13 bacteriophage, (b) TMV, (c) HPV, and (d) HIV. In each figure, the first vial corresponds to the control and the second one represents laser-irradiated sample. All the data are expressed in the form of mean±standard deviation.

2.0 mM $MgCl_2$, and 0.4 mg/ml X-gal. Cells positive for β-galactosidase activity were counted manually (sum of 10 fields, duplicate samples).

2.2.4 *For TMV*

Tobacco mosaic viruses from the infected tobacco leaves were extracted and used as the source of virus in our experiments. The atomic force microscope (AFM) images showing the release of single-strand RNA from TMV were used as an indication of the inactivation.

2.3 *Imaging Viruses with Atomic Force Microscope*

Biomolecules such as protein, DNA and RNA can be easily captured on the APTES (Aminopropyltriethoxysilane)-modified surface using glutaradehyde. The laser-irradiated viral particles were immobilized on the APTES mica and imaged[5–8] under the AFM.

2.3.1 *APTES mica preparation*

Fresh cleaved mica was placed in a desiccator with 30 μl APTES (99%, Sigma-Aldrich, St. Louis, Missouri) and 10 μl N,N-diisopropylethylamine (99%, distilled, Sigma-Aldrich) in the bottom. The desiccator was then purged with argon for 3 min, and the mica was allowed to remain in the APTES vapor for 1 h to achieve good modification.

2.3.2 *Sample immobilization*

One hundred microliters of 2 μM glutaradehyde (grade I, Sigma-Aldrich) was deposited onto the APTES mica surface for 10 min, and the surface was then washed gently with distilled water. After that, 200 μl of virus samples with concentration range from 1×10^6 to 1×10^8 particles per milliliter was pipetted onto the glutaradehyde-treated mica surface and allowed to incubate for 40 to 80 min. The mica surface, now containing the immobilized sample, was then gently rinsed with distilled water and dried with nitrogen.

2.3.3 *Imaging*

Imaging was carried out with a PicoPlus 2500+ AFM [Molecular Imaging; now 5500 AFM (N9410S) from Agilent] equipped with a Si_3N_4 cantilever (AppNano SPM) with a spring constant range from 25 to 75 N/m and the resonance frequency around 300 kHz

3 Experimental Results

3.1 *Inactivation of M13 Bacteriophages*

Figure 2(a) shows the number of plaques of two typical assays for a sample with 1×10^3 pfu of M13 bacteriophages without the laser irradiation (control) and with laser irradiation. The laser power density used was 100 ± 10 MW/cm^2. The number of plaques was determined to be 990 ± 49 counts for the

control. In contrast, the number of plaques after laser irradiation was 3 ± 2 counts. The important feature is that there is a minimal number of plaques for the laser irradiated sample as compared with the control, indicative of the very efficient inactivation of M13 bacteriophages by the ultrashort pulsed (USP) laser irradiation. A viral load reduction of about 10^3 was observed.

3.2 Inactivation of TMV

The assay of TMV was performed by counting the single-stranded RNA released in the laser-irradiated sample with AFM, i.e., one count of single-stranded RNA observed in the AFM image corresponds to inactivation of one TMV in the laser irradiated sample. Figure 2(b) shows the number of TMV particles in the control and laser-irradiated samples, respectively. The control had 105 ± 6 TMV particles, whereas the laser-irradiated sample had 44 ± 3. The laser power density employed was 900 ± 90 MW/cm^2. USP laser irradiation reduced the viral load by a factor of about 55%.

3.3 Inactivation of HPV

The inactivation of HPV was determined from SEAP assays. Figure 2(c) shows the number of HPV particles for the control and laser-irradiated samples, respectively. The control had 9980 ± 400 HPV particles and the laser-irradiated sample had 2 ± 1. The laser power density used was 1.0 ± 0.1 GW/cm^2. A viral load reduction of about 10^4 was recorded.

3.4 Inactivation of HIV

The inactivation of HIV was assayed by monitoring the infectivity of U373-MAGI-CXCR4$_{CEM}$ cells. Figure 2(d) shows the number of infected cells—an indicator of the number of HIV—for the control and laser-irradiated HIV samples, respectively. The laser power density used in the experiments was 1.1 ± 0.1 GW/cm^2. The control sample revealed infection of 60 ± 3 CD4$^+$ T cells; whereas the laser-irradiated sample shows 12 ± 1. A reduction of viral infectivity of about 80% was observed.

3.5 Images from Atomic Force Microscopy

M13 bacteriophage is a rod-shaped virus with a diameter of about 6 nm and a length of about 850 nm. Its capsid is made up of proteins assembled in helical shape and wrapped around a single-stranded DNA. Figures 3(a) and 3(b) show AFM images of M13 phage without and with laser irradiation, respectively. The laser power density used was 200 ± 20 MW/cm^2. The wormlike features in Fig. 3(a) reveal the presence of M13 bacteriophages in the control. Nearly all the wormlike features disappear and are replaced by mucuslike structures after laser irradiation [Fig. 3(b)], indicative that the laser irradiation affects the global structure of the viral capsid coat.

TMV is a rod-shaped virus whose length can vary depending on the method of extraction. On average, it has a length of about 300 nm, a diameter of about 18 nm, and contains a single-stranded RNA. The rectangular white structures correspond to AFM images of TMV in the control [Fig. 3(c)]. The very narrow wormlike features, which show up only in the laser-irradiated sample [Fig. 3(d)], represent single-stranded RNAs released from the TMV, presumably as a result of huge

vibrations of the TMV protein shell coherently excited by the laser, as discussed in the following. The laser power density used was 1.0 ± 0.1 GW/cm^2.

Therefore, AFM images for M13 bacteriophages and TMV have clearly demonstrated that USP laser irradiation can affect the structural integrity of the capsid of a virus.

Imaging the laser-irradiated samples for both HPV and HIV with the AFM is being planned. These experiments, which can provide valuable information about the effects of laser irradiation, are challenging because of the highly infectious properties of the viruses.

3.6 Inactivation of Both the Wild and Genetically Modified M13 Bacteriophages

We have also carried out wild-type M13 bacteriophages in addition to the interference-resistant helper phages already shown. These results indicate that the threshold laser power intensities for inactivation of M13 bacteriophage and M13 interference-resistant helper phage are the same (within the experimental uncertainty). These experimental results suggest that our method can overcome limitations with current therapeutics that arise due to mutations. We believe that this novel property of our method is due to the fact that the excited coherent acoustic vibrations induced in the capsids of M13 phages are usually of long wavelength. As a result, they are relatively insensitive to the minor local changes such as those due to mutations.

3.7 Efficiency of the Method

Figure 4 shows the number of plaques as a function of the laser exposure time for a M13 bacteriophage sample. The laser power density used was 100 ± 10 MW/cm^2. The inactivation is approximately exponential with a time constant of about 0.2 h. The number of viral particles was reduced to less than about 10% after 0.5 h of exposure to laser irradiation, and to less than about 0.5% after 1 h of laser exposure time. We have found that the efficiency of inactivation depends on how efficiently the viral particle was placed within the effective volume of the near-IR subpicosecond fiber laser within the vial. More efficient magnetic stirring gives rise to more efficient inactivation.

3.8 Selective Inactivation

We now evaluate the effects of the near-IR subpicosecond fiber laser light on other microorganisms besides viruses. Table 1 summarizes the threshold laser power density for inactivation of a variety of microorganisms, including human red blood cells, human Jurkat cells, and mouse dendritic cells. Much higher laser power intensities are necessary to inactivate these cells. These results indicate that there exists a window in laser power density (or equivalently, laser intensity because the same laser was used for the experiments), which was bounded approximately by 1 GW/cm^2 and 10 GW/cm^2, that enables us to inactivate unwanted microorganisms such as viruses, while leaving useful materials like mammalian cells unharmed.

It is therefore plausible that the near-IR subpicosecond fiber laser, if appropriately manipulated, can be used to selectively kill blood-borne pathogens with minimal damage to sensitive materials. It is this selectivity of our method that
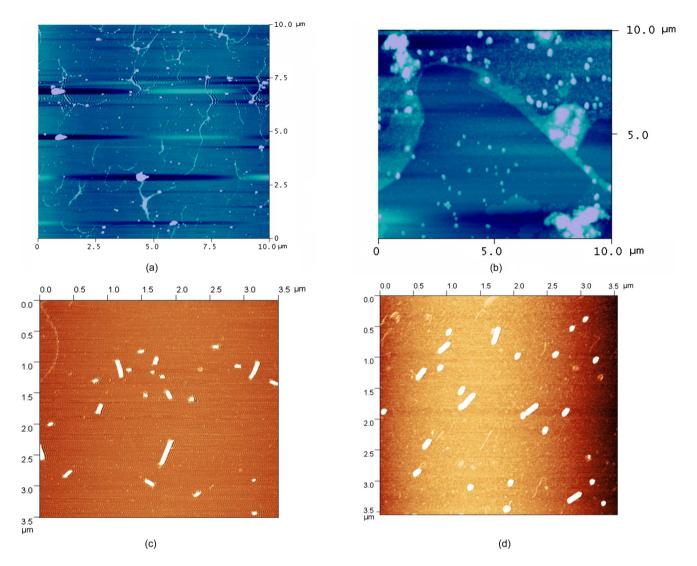
Fig. 3 AFM images of (a) M13 bacteriophage sample without laser irradiation (control); (b) M13 bacteriophage sample with laser irradiation; (c) TMV sample without laser treatment (control), and (d) TMV sample with laser irradiation. The laser power density used for M13 bacteriophage was 200 ± 20 MW/cm^2. The laser power density used for TMV was 1.0 ± 0.1 GW/cm^2. The wormlike features in (a) reveal the presence of M13 bacteriophages in the control. In (b), nearly all the wormlike features disappear and are replaced by mucuslike structures after laser irradiation, indicative that the laser irradiation affects the global structure of the viral capsid coat. The rectangular white structures correspond to AFM images of TMV in (c). The very narrow wormlike features, which show up only in the laser-irradiated sample in (d), represent single-stranded RNAs released from the TMV, presumably as a result of huge vibrations of the TMV protein shell coherently excited by the near-IR subpicosecond fiber laser.

distinguishes our approach from currently available methods. Our photonic approach has great potential to be used for the disinfection of viral pathogens in blood products and for the treatment of blood-borne viral diseases performed as a dialysis process in the clinic with minimal side effects.

3.9 Dependence of Inactivation on the Excitation Laser Power Density

Figure 5 shows the dependence of inactivation of a M13 bacteriophage sample on the power density of excitation laser. The laser exposure time was kept at 10 h. When the power density was lower than about 40 MW/cm^2, no inactivation was observed within the experimental uncertainty; however, as the power density was increased to 60 MW/cm^2 and higher, inactivation was seen to occur. The abrupt separation
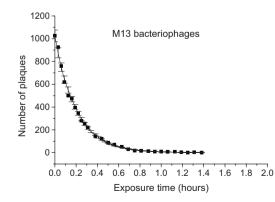

Fig. 4 Number of plaques for a M13 bacteriophage sample as a function of the exposure time to radiation by a near-IR subpicosecond fiber laser. All the data are expressed in the form of mean±standard deviation.

Table 1 Threshold laser power density for inactivation of viruses and cells.

	Viruses and Cells						
	M13	TMV	HPV	HIV	Human Red Blood Cell	Human Jurkat T Cell	Mouse Dendritic Cell
Threshold laser power density for inactivation (GW/cm^2)	0.06	0.85	1.0	1.1	15	22	12

of laser power density around 60 MW/cm^2 for the inactivation of M13 bacteriophage was consistent with the argument that damage on the capsid was the cause of inactivation.

4 Discussion

One can obtain a very valuable hint about the likely mechanism(s) for the inactivation of viruses with an USP laser from the AFM images presented here for M13 bacteriophages and TMV. The AFM images from Figs. 3(a)–3(d) strongly suggest that the probable mechanism for inactivation of viruses by the near-IR subpicosecond fiber laser is concomitant with laser-induced damage of the capsid.

To our knowledge, there are three possible mechanisms in which an USP laser can produce vibrational motions on either a solid state system or a biological molecular system. One possible physical mechanism of inactivation of a virus is direct excitation of vibrational Raman-active modes on the capsid of a virus by a near-IR subpicosecond fiber laser through the impulsive stimulated Raman scattering (ISRS) process.[9–22] If the amplitude of the vibrations is large enough to break the weak links (presumably the hydrogen bonds) between the proteins, damage to the capsid of the virus occurs, leading to viral inactivation. However, we estimate that a single laser pulse from the USP laser used in our experiment probably can not generate large enough vibrational amplitude on the protein coat of a viral particle to break the weak hydrogen bonds (for example, if we use a Raman scattering cross section for a typical molecule and assume that the vi-
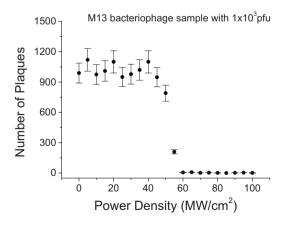
brational frequency of 1 GHz, then the amplitude of the excitation is estimated to be of the order of 10^{-1} Å); rather, multiple laser pulses are required. Qualitatively, this is how it might work with multiple laser pulses. Let us assume that the links between the proteins of a capsid can be simulated with springs of given spring constants. The first laser pulse interacting with the capsid excites a tiny amplitude of vibration on the capsid. Because of the polar nature of water surrounding the capsid, it effectively screens the hydrogen bonds and as a result it softens the spring constants: Therefore, when the subsequent second laser pulse interacts with the excited capsid, the amplitude of the vibration on the excited capsid will be a little bit larger than that excited by the first laser pulse. This same argument can be applied for hundreds, thousands, or millions times depending on the experimental conditions. Our preliminary results, which indicate that it takes some time to inactivate viral particles, seem to be consistent with this scenario.

The other possible mechanism is the indirect generation of vibrations on the capid of a virus through electronic absorption of the laser radiation. Under this scenario, photons are first absorbed by the viral particles through electronic excitations to the higher electronic states. These energetic electronic states relax toward the ground state by giving off energy to vibrational states on the capsid of the viral particles, damaging the capid, and leading to the inactivation.

The third likely mechanism is the generation of a shock wave by the USP laser. A USP laser has been known (see Ref. 23 and the references therin) to produce a shock wave when interacting with materials including biological molecules.

Note that the specific mechanism accounting for our experimental results of inactivating viral particles with USP lasers is not known at this time. More work is required to clarify the possible mechanisms described here.

Note that the reason why there exists a window in laser power density that allows the selective inactivation of viruses, as demonstrated in Table 1, is not known at this moment. One likely reason is the difference in the structure. We know that the structure of the lipid membrane on the cell is significantly different from that of the capsid of a viral particle. This structural difference might play a role in the interpretation. Another likely reason is the size effects. Viral particles are typically much smaller than mammalian cells. For example, HIV is an enveloped virus with a capsid and is about 0.1 μm in diameter; whereas the shape of a human red blood cell is like a donut, about 10 μm in diameter and 2 μm in thickness. The mouse dendritic cell is about 10 μm in diameter. Since the

Fig. 5 Number of plaques for a M13 bacteriophage sample as a function of the excitation laser power density. The inactivation was seen to occur rather sharply at around 60 MW/cm^2.

viruses and cells are embedded in water, the water molecules play a crucial role in the damping of the vibrations excited by the laser. The relatively large size of either the human red blood cell or the mouse dendritic cell as compared with that of the viral particle means that there are more water molecules surrounding the red blood cells and dendritic cells than HIV; in other words, the damping associated with the coherent/incoherent excitation created by the laser is less for HIV than for red blood cells or dendritic cells. As a result, the amplitude of vibrations created by a given laser power density can be much higher for HIV than for red blood cells or mouse dendritic cells.

It is obvious that if the laser causes the nucleic acid to leave a virus, as was shown in the AFM images of laser-irradiated TMV sample in Fig. 3(d), damage to the virus has been produced. However, TMV can also become inactivated even with its RNA intact due to damage to its protective capsid. Consequently, the assay result—a 55% load reduction by laser irradiation (which used the release of RNA as an indicator for inactivation of TMV)—represents a lower bound value.

Our experiments show that the near-IR subpicosecond fiber laser can reduce about 80% of the viral load in HIV samples. This is not sufficient by clinical standards for therapeutic purposes. However, we notice that the relatively small viral load reduction observed in our experiments is actually a manifestation of the use of a magnetic stirrer as well as the limitation imposed on the duration of the laser-irradiation time. If a more efficient way were used to get the photons in the laser beam to interact with the viral particles, then more efficient inactivation of viruses would have been achieved.

5 Conclusion

We demonstrated that a near-IR subpicosecond fiber laser can be used to selectively inactivate viral particles ranging from nonpathogenic viruses such as M13 bacteriophage and TMV to pathogenic viruses such as HPV and HIV, while leaving sensitive materials like human Jurkat T cells, human red blood cells, and mouse dendritic cells unharmed. This photonic approach targets the global mechanical properties of the viral protein shell, making it relatively insensitive to the local genetic mutation in the target viruses. As a result, the approach can inactivate both the wild and mutated strains of viruses. This intriguing advantage is particularly important in the treatment of diseases involving rapidly mutating viral species such as HIV. This USP laser technology could be used for the disinfection of viral pathogens in blood products and for the treatment of blood-borne viral diseases in the clinic.

References

1. K. Rosenheck and P. Doty, "The far ultraviolet absorption spectra of polypeptide and protein solutions and their dependence on conformation," *Proc. Natl. Acad. Sci. U.S.A.* **47**(11), 1775–1785 (1961).
2. J. C. Sutherland and K. P. Griffin, "Absorption spectrum of DNA for wavelengths greater than 300 nm," *Radiat. Res.* **86**, 399–410 (1981).
3. B. J. Bryant and H. G. Klein, "Pathogen inactivation: the definitive safeguard for the blood supply," *Arch. Pathol. Lab Med.* **131**, 719–733 (2007).
4. Center for Cancer Research, "Constructions and detailed protocols for the preparation of the pseudovirions," Laboratory of Cellular Oncology Technical Files, http://home.ccr.cancer.gov/lco/default.asp.
5. H. D. Wang, R. Bash, J. Yodh, G.Hagar, D.Lohr, and S.Lindsay, "Glutaraldehyde modified mica: a new surface for atomic force microscopy of chromatin," *Biophys. J.* **83**, 3619–3625 (2002).
6. X. Ji, J. Oh, A. K. Dunker, and K. W. Hipps, "Effects of relative humidity and applied force on atomic force microscopy images of the filamentous phage fd," *Ultramicroscopy* **72**, 165–176 (1998).
7. K. T. Nam, B. R. Peelle, S. W. Lee, and A. M. Belcher, "Genetically driven assembly of nanorings based on the M13 virus," *Nano Lett.* **4**, 23–27 (2004).
8. D. Anselmetti, R. Luthi, E. Meyer, T. Richmond, M. Dreier, J. E. Frommer, and H. J. Guntherodt, "Attractive-mode imaging of biological materials with dynamic force microscopy," *Nanotechnology* **5**, 87–94 (1994).
9. Y.-X. Yan, E. B. Gamble, Jr, and K. A. Nelson, "Impulsive stimulated scattering: general importance in femtosecond laser pulse interactions with matter, and spectroscopic applications," *J. Chem. Phys.* **83**, 5391–5399 (1985).
10. K. A. Nelson, R. J. D. Miller, D. R. Lutz, and M. D. Fayer, "Optical generation of tunable ultrasonic waves," *J. Appl. Phys.* **53**, 1144–1149 (1982).
11. S. De Silvestri, J. G. Fujimoto, E. P. Ippen, E. B. Gamble, Jr., L. R. Williams, and K. A. Nelson, "Femtosecond time-resolved measurements of optic phonon dephasing by impulsive stimulated raman scattering in α-perylene crystal from 20 to 300 K," *Chem. Phys. Lett.* **116**, 146–152 (1985).
12. K. A. Nelson, "Stimulated Brillouin scattering and optical excitation of coherent shear waves," *J. Appl. Phys.* **53**, 6060–6063 (1982).
13. G. C. Cho, W. Kutt, and H. Kurz, "Subpicosecond time-resolved coherent-phonon oscillations in GaAs," *Phys. Rev. Lett.* **65**, 764–766 (1990).
14. T. K. Cheng, J. Vidal, H. J. Zeiger, G. Dresselhaus, M. S. Dresselhaus, and E. P. Ippen, "Mechanism for displacive excitation of coherent phonons in Sb, Bi, Te, and Ti2O3," *Appl. Phys. Lett.* **59**, 1923–1925 (1991).
15. J. M. Chwalek, C. Uher, J. F. Whittaker, and G. A. Mourou, "Subpicosecond time-resolved studies of coherent phonon oscillations in thin-film YBa2Cu3O6+x ($x<0.4$)," *Appl. Phys. Lett.* **58**, 980–982 (1991).
16. R. Merlin, "Generating coherent THz phonons with light pulses," *Solid State Commun.* **102**, 207–220 (1997).
17. K. T. Tsen, S.-W. D. Tsen, C.-L. Chang, C.-F. Hung, T. C. Wu, and J. G. Kiang, "Inactivation of viruses by coherent excitations with a low power visible femtosecond laser," *Virology J.* **4**(50), 1–5 (2007).
18. K. T. Tsen, S.-W. D. Tsen, C.-L. Chang, C.-F. Hung, T. C. Wu, and J. G. Kiang, "Inactivation of viruses with a very low power visible femtosecond laser," *J. Phys.: Condens. Matter* **19**, 322102 (2007).
19. K. T. Tsen, S.-W. D. Tsen, C.-L. Chang, C.-F. Hung, T. C. Wu, and J. G. Kiang, "Inactivation of viruses by laser-driven coherent excitations via impulsive stimulated Raman scattering process," *J. Biomed. Opt.* **12**, 064030 (2007).
20. K. T. Tsen, S.-W. D. Tsen, O. F. Sankey, and J. G. Kiang, "Selective inactivation of microorganisms with near-infrared femtosecond laser pulses," *J. Phys.: Condens. Matter* **19**, 472201 (2007).
21. Y. R. Shen and N. Bloembergen, "Theory of simulated Brillouin and Raman scattering," *Phys. Rev.* **137**, A1787–A1805 (1965).
22. Y. R. Shen, *The Principles of Nonlinear Optics*, Wiley, New York (1984).
23. M. Boustie, L. Berthe, T. de Resseguier, and M. Arrigoni, "Laser shock waves: fundamentals and applications," *Proc. 1st Int. Symp. on Laser Ultrasonics: Science, Technology and Applications*, paper #2, National Research Council of Canada, Montreal (2008).